

THE FORMULATION AND EVALUATION OF 6-THIOGUANINE AS A NANOSTRUCTURE LIPID CARRIER FOR THE TARGETED DELIVERY OF BREAST CANCER

ALAA A. HASHIM^{1*}, DHIYA ALTEMEY², HUSSEIN ABDELAMIR MOHAMMAD³, HASANAIN SHAKIR MAHMOOD⁴, RADHWAN M. HUSSEIN¹, MAHSA REZAEI⁵, PEGAH KHOSRAVIAN⁶

¹Pharmaceutics Department, College of Pharmacy, Ahlul-Bayt University, Karbala, Iraq. ²Department of Pharmaceutics, College of Pharmacy, Al-Zahraa University for Women, Karbala, Iraq. ³Pharmaceutics Department, College of Pharmacy, University of Al-Qadisyah, Al-Qadisyah, Iraq. ⁴University of Alkafeel–College of Pharmacy, Al-Najaf, Iraq. ⁵Faculty of Pharmacy, Tehran University of Medical Sciences, Tehran, Iran; Department of Pharmaceutical Nanotechnology, Faculty of Pharmacy, Tehran University of Medical Sciences, Tehran, Iran. ⁶Medical Plants Research Centre, Basic Health Sciences Institute, Shahrekord University of Medical Sciences, Shahrekord, Iran
*Corresponding author: Alaa A. Hashim; *Email: almadinah006@yahoo.com

Received: 14 Jan 2024, Revised and Accepted: 05 Mar 2024

ABSTRACT

Objective: The main goal was to avoid all the problems associated with usual breast cancer treatment by using 6-thioguanine as a nanostructure lipid carrier (TG-NLCS). This was accomplished by administering an effective and targeted dose of 6-thioguanine (TG) to the tumour site using a long-lasting and biodegradable delivery system.

Methods: A combination of heat homogenization and ultrasonication was used to implement the emulsification process. To obtain the optimal formulation, the prepared formulations were first assessed for particle size, Polydispersity Index (PDI), zeta potential, entrapment efficiency, and drug loading capacity. Additionally, a range of physicochemical characterization techniques were employed, including dissolution studies, melting point determination, Fourier-Transform Infrared (FTIR) spectroscopy, and Field Emission Scanning Electron Microscopy (FESEM), as well as cytotoxicity assessment of TG-NLCS in MCF-7 breast cancer cells.

Results: The selected formula, TG03, showed a zeta potential of -13.5 ± 0.27 mV and a particle size of 149 ± 0.55 nm. This was further examined using a FESEM. In the *in vitro* drug release study, the formula demonstrated better-controlled drug release for 48 h in comparison to other formulations. In addition, the significant anti-proliferation activity of TG-NLCS against the MCF-7 breast cancer cell line.

Conclusion: Nanostructured lipid carriers (NLCs) are one type of multifunctional nanoparticle that includes many combinations of lipids and medicines for various delivery routes.

Keywords: Breast cancer, Thioguanine (TG), Nanostructured lipid carriers (NLCs), Polydispersity index, Zeta potential

© 2024 The Authors. Published by Innovare Academic Sciences Pvt Ltd. This is an open access article under the CC BY license (<https://creativecommons.org/licenses/by/4.0/>)
DOI: <https://dx.doi.org/10.22159/ijap.2024v16i3.50379> Journal homepage: <https://innovareacademics.in/journals/index.php/ijap>

INTRODUCTION

Nanotechnology-based drug delivery systems are now being utilised as effective approaches not only to improve therapeutic efficacy but also to reduce the adverse reactions of cancer chemotherapy [1].

Chemotherapy is a fundamental form of treatment for cancer patients. The major challenge in breast cancer chemotherapy has been the deleterious impact of anticancer medications on healthy cells and the resistance of some patients to respond to treatment [2].

Thioguanine (also known as 6-thioguanine and tioguanine) is a purine antagonist and an anticancer medication that operates by affecting DNA and RNA. It is quite beneficial in children with acute leukaemia, choriocarcinoma, and solid malignancies. It destroys cells with extraordinarily fast growth kinetics without differentiating between normal and abnormal cells.

Thioguanine (TG) is a pale yellow, crystallised powder that is essentially insoluble in water, alcohol, and chloroform but dissolves in dilute alkali hydroxide solutions. It has a molecular weight of 167.2 g/mol and a molecular formula of $C_5H_5N_5S$. The TG chemical structure [3] is shown in fig. 1.

Notwithstanding its use in cancer chemotherapy, the purine derivative has been linked to several adverse effects [4]. People who have a hereditary impairment in the thiopurine S-methyltransferase enzyme are at increased risk of adverse effects [5].

There are many approaches for decreasing or avoiding treatment side effects. Loading TG into NLCs is one effective method for overcoming the adverse reactions of this anticancer medication [6]. NLCs are now recognised as a promising candidate in the treatment of cancer,

suggesting that they provide a versatile base for the delivery of medicines [7].

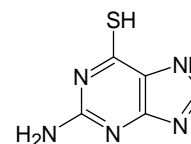


Fig. 1: Displays the chemical structure of thioguanine [8]

MATERIALS AND METHODS

The procurement of TG was conducted through the acquisition of Hangzhou Hyper Chemicals Limited. Miglyol®812 was procured from Merck and IOI Oleo (Germany), whereas Cetyl Palmitate (CP), Poloxamer 188 (P188), Lecithin from Soybean, Vitamin E Polyethylene Glycol Succinate, Tween®80, and Compritol® 888 ATO were obtained from HyperChem®, Zhejiang, China. The MCF-7 cell line, derived from human breast cancer cells, was obtained from the National Cell Bank of Iran, located at the Pasteur Institute of Iran in Tehran.

Method

The melting point of drug

The melting point of the drug powder was determined using an electrical melting point instrument and the capillary tube technique, as specified by the USP. A 10 cm long and 1.2 mm internal diameter capillary tube was dipped in the drug powder,

closed from one end, and put inside the melting point device, where the temperature was gradually raised. The temperature at which the medication powder changed from solid to fluid was measured at the melting point [9].

Determination of maximum absorbance of drug

To ascertain the maximal absorbance (ϵ_{\max}) of the medicine, to make a solution, 10 mg of the medication was dissolved in one millilitre of dimethyl sulfoxide (DMSO). Within the region of 200–400 nm using UV-Vis spectroscopy, the ultraviolet spectra of one mg per ml solution in DMSO were studied to determine what elements were present [10].

Preparation of the calibration curve

Calibration curves of TG in DMSO solutions were constructed by preparing serial dilutions of TG with different concentrations of 5–25 $\mu\text{g}/\text{ml}$ from a concentration that is stored as a stock solution of 1000 $\mu\text{g}/\text{ml}$. Samples were analysed spectrophotometrically at the wavelength of maximum absorbance of TG. The measured absorbances were recorded and plotted versus the respective concentrations [11].

Preparation of nanostructured lipid carriers

To prepare NLCs in the same way as before, the emulsification and solvent evaporation processes were applied [12]. The oily phase consisted of TG, a mixture of liquid and solid lipids. On the other hand, the composition of the aqueous phase was a blend of surfactant and co-surfactant in deionized water [13]. The mixtures were subsequently introduced into a sonicator bath set at a temperature of 25 °C and subjected to sonication on five occasions, each lasting five minutes. The sonication process was carried out using a probe-type ultrasonicator (Misonix S-4000 Sonicator, USA) at an amplitude of 50%, with an interval of eight seconds between each sonication cycle.

This procedure aimed to generate a finely dispersed emulsion. The oil phase and an aqueous stage were preheated individually to a temperature of 75 °C before carrying out this procedure. Subsequently, the oil phase was carefully transferred into the aqueous phase dropwise. Subsequently, the pH of the formulations was modified to 7.4 by employing 1N NaOH. The resulting precipitated TG was eliminated from the solution through filtration using a membrane filter with a pore size of 0.45 micrometres. At a temperature of four degrees Celsius, the formulations were kept in containers that were airtight and shielded from light [14]. In this particular investigation, the type of sterilisation that was carried out was membrane filtration sterilisation (the experiment was conducted with a membrane filter featuring a pore diameter of 0.22 microns) [15].

Analysis of the size distribution of nanoparticles

The particle size, polydispersity index, and zeta potential of TG-NLCs were determined using a Zetasizer-ZS instrument manufactured by Malvern Instrument (UK). Subsequently, measurements were taken for the mean of particle sizes, polydispersity index, and standard deviations of zeta potential. To prevent the agglomeration of particles, measurements were conducted repeatedly [16].

Drug entrapment efficiency and drug loading capacity

Indirectly, we were able to compute the entrapment efficiency (%EE) in addition to the drug loading capacity (%DL) by evaluating the unbound TG in the NLCs. These percentages correspond to the amount of TG successfully encapsulated in the NLCs. The concentration of unbound drug that was not captured was calculated using an ultrafiltration method. In this experiment, a volume of 5.0 ml of TG-NLC solution was introduced into the ultra-centrifugal tube (MWC0 of 10 kDa).

The tube was then subjected to centrifugation at a speed of 5,000 rpm for 30 min. Ultrafiltration with free drug and untrapped TG concentrations was analysed using UV-Vis spectroscopy. The equations used to determine the %EE and the DL% are as follows:

$$\%EE = \frac{W_T - W_F}{W_T} \times 100 \dots\dots (1)$$

$$\%DL = \frac{W_T - W_F}{W_L} \times 100 \dots\dots (2)$$

Where the weighted total (WT) refers to the overall weight of the drug being analysed. The weight-free (Wf) represents the amount of drug that is discovered in the supernatant after the aqueous dispersion has undergone ultrafiltration. Lastly, the weight of the lipid (WL) corresponds to the weight of the lipid used in the experiment [17].

Fourier-transform infrared spectroscopy

To investigate any potential interactions between TG and other excipients and to confirm the drug's identification, FTIR spectroscopy (FTIR-8400S, Shimadzu, Japan) was utilised. Spectroscopic analysis was conducted on both the isolated drug compound and various physical mixtures of the drug and lipids. Every individual sample was accurately measured and processed on a potassium bromide (KBr) disc [18]. The spectrum was subjected to scanning with a frequency resolution ranging from 400 to 4000 cm^{-1} .

Field emission scanning electron microscope

The FESEM instrument used in this study was the Hitachi S-4160, manufactured in Japan. It was employed to get topographic and fundamental data for the selected formula (TG03). The scanning electron microscope electron gun's field-emission cathode produces narrower beams at higher and lower electron energies; this leads to a higher temporal resolution and reduced sample loading and degradation. In the context of applications that necessitate the utilisation of the largest feasible aperture [19].

A study on cell culture

MCF-7, a human breast cancer cell line was cultured in DMEM supplemented with 10% FBS (foetal bovine serum) and 1% penicillin/streptomycin at 37 °C in a humidified atmosphere with 5% CO_2 . The cells were trypsinized, resuspended in complete media (DMEM with FBS and antibiotics), and counted at 80% confluence to determine cell density. A phase-contrast microscope (Olympus CKX41) was used to evaluate the overall appearance of the cells. Microphotographs were obtained with objectives 4 and 10, respectively [20].

Cytotoxicity assay

MCF-7 cells were inoculated into a 96-well plate with a cellular density of 2×10^4 cells per well. The cell culture medium was replaced with medicine at concentrations of 0, 0.1, 0.5, 1, 5, 10, 50, and 100 $\mu\text{g}/\text{ml}$ after 24 h of incubation. After 72 h, the supernatants were subjected to extraction. Subsequently, a volume of 50 μl of fresh Dulbecco's Modified Eagle Medium (DMEM) was introduced into each well, along with an additional 50 μl of 5-mg/ml 3-(4,5-dimethyl thiazolyl)-2,5-diphenyltetrazolium bromide (MTT). The resulting mixture was then incubated for a duration of 3 to 4 h at a temperature of 37 °C within a controlled environment, including 5% carbon dioxide (CO_2) and adequate humidity.

Afterwards, 150 μl of dimethyl sulfoxide (DMSO) was introduced into each well with agitation for 15 min. The absorbance measurement was conducted at a wavelength of 570 nm with a microplate reader (Biotec, Tecan US, Inc.). The viability of the treatment groups was reported as the percentage of controls, which was set at 100%. The mean and the standard error of the mean (SEM) of cell viability for each treatment were determined [21]. The following formula calculates the cell viability (%):

$$\text{Cell viability (\%)} = \left[\frac{A_s}{A_c} - \frac{A_b}{A_b} \right] \times 100 \dots\dots\dots (3)$$

The variables denoted as "As," "Ac," and "Ab" represent the absorbance values of the experimental wells, control wells, and blank wells, respectively [22].

IC₅₀ determination

The current investigation sought to investigate the cytotoxic impacts of three distinct concentrations of the substance. (1, 2, and 5 $\mu\text{g}/\text{ml}$) of both free drugs and manufactured drugs on MCF-7 cells. The cytotoxicity was assessed using the MTT test. The control cells were

cultivated concurrently in a standard medium, specifically, Dulbecco's Modified Eagle Medium (DMEM) supplemented with 1% antibiotic penicillin/streptomycin, for 72 h. In addition, the biocompatibility of the drug carrier was evaluated through the treatment of cells with a polymer devoid of any medication [23].

In vitro drug release study

The *in vitro* release experiments of NLC took place with the use of a dialysis bag molecular weight cut-off (MWCO 8000–12000, Viskase Companies, USA), which was previously submerged in a dissolving medium for an entire night.

The receptor medium and sink conditions were established using fifty millilitres of a buffer containing phosphate with a pH of 7.4. In the dialysis bag, one millilitre of the NLC was put, and the incubator agitator was used to agitate the dialysis bag at a speed of 100 ± 2 revolutions per minute (rpm) while keeping the temperature of the medium at 37 ± 0.5 °C.

The sample that was withdrawn and the quantity of TG released in each sample were determined by the use of a UV-Vis spectroscopy set at a wavelength of 348 nm. A count of the total amount of medication that was discharged was determined. The values that have been reported are the averages of three separate replicates [24].

Statistical analysis

The results of the experimental study were presented as the mean of triplicate models \pm standard error of the mean (SEM). These results

were analysed using a one-way analysis of variance (ANOVA) to assess the statistical significance of the changes in applied factors. A significance level of ($P < 0.05$) was used to determine if the observed changes were statistically significant, while a significance level of ($P > 0.05$) indicated non-significance [25].

RESULTS AND DISCUSSION

Drug characterization

The drug melting point was measured by an electrothermal melting point apparatus according to USP and was 365 °C. This result was aligned with the reported values [26] that might indicate the purity of the powder sample used in the study [27].

The drug was scanned in DMSO with UV-Vis spectroscopy at a concentration of 150 $\mu\text{g/ml}$ at 200–400 nm, with the peak showing the λ_{max} of 348 nm. The melting point and λ_{max} , according to USP, confirm the label on the drug sample of thioguanine [9].

The calibration curve of TG

The thioguanine calibration curve in dimethyl sulfoxide (DMSO) is shown in fig. 2. The plotting of absorbance against concentrations resulted in a straight line. The square correlation coefficients (R^2) were 0.999. This means that the calibration curve complies with the law of Beer in the range of concentrations used.

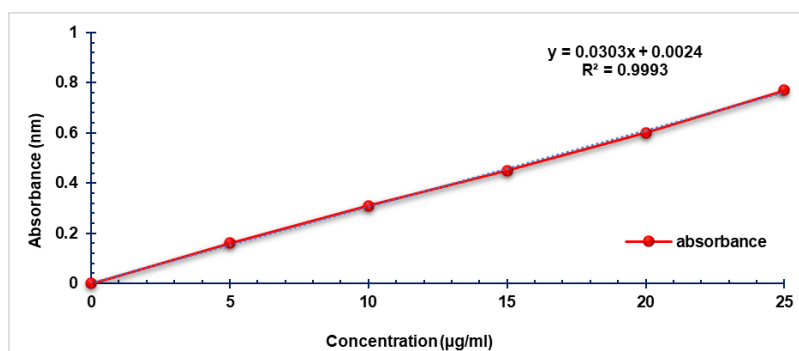


Fig. 2: Displays the calibration curve of thioguanine in dimethyl sulfoxide

The process of preparing TG-NLCs

The study presents five formulations of TG-NLCs (TG01-TG05) as outlined in table 1, which aim to have a heightened therapeutic impact while simultaneously reducing adverse effects. The experimental procedure involved the incorporation of a lipid combination consisting of both solid and liquid lipids, together with a drug compound, into an organic solvent. This mixture was subsequently emulsified in an aqueous phase. The melting lipid phase was added to the aqueous phase at a rate of approximately 1 ml per minute in a dropwise manner. Following the process of

solvent evaporation, the lipid undergoes precipitation, resulting in the formation of NLCs.

The organic solvent serves as the solvent for the chemotherapy drug, facilitating its dissolution. Subsequently, the resulting NLCs, which contain the drug, can be dried without the requirement of additional NLC preparation at high temperatures. Moreover, the efficacy of this procedure is constrained by the existence of residual hazardous compounds within the outcome, potentially resulting in systemic toxic manifestations after administration [28].

Table 1: The composition of the nanostructured lipid carriers formulations loaded with TG

Formula	TG (mg)	CP (mg)	Compritol (mg)	Miglyol®812 (mg)	TPGS (mg)	Lecithin (mg)	P188 (mg)	Tween®80 (mg)	DW (ml)
TG01	40	100	100	35	5	10	5	10	100
TG02	40	150	50	35	5	10	5	10	100
TG03	40	50	150	35	5	10	10	10	100
TG04	40	50	150	35	5	10	5	10	100
TG05	40	50	150	35	5	10	10	5	100

TG-Thioguanine, CP-Cetyl palmitate.

Particle size distribution and polydispersity index

NLCs are classified depending on their size, form, and loading capacity. In this work, NLCs were generated using the previously reported approach [29], and FSEM was used to establish their size and shape. The cellular absorption of NLCs is greatly influenced by particle size and shape [30]; as a result, spherical forms are the best options for efficiently eliminating cancer cells [31]. Smaller sizes are thought to be less toxic [30].

The TG-NLCs were synthesised using a specific formula, and the particle sizes observed were found to be in the submicron range, as indicated in table 2 and fig. 3. The particle size assessment plays a critical role in the characterization of lipid nanoparticles, as it directly impacts the ratio of Compritol® 888 ATO (glyceryl behenate) and Cetyl Palmitate (CP) with Poloxamers 188.

Poloxamers have also been shown to sterically stabilise nanoparticles and limit the adsorption of plasma proteins or opsonin on the surface of nanoparticles by imparting a hydrophilic feature to the surface of nanoparticles, hence preventing the clearance of drugs containing LNPs from circulation [32].

The stable NLCs would also provide a longer shelf life and reduce noxiousness. Site-specific NLCs, specifically those recommended, should be carriers of chemotherapeutic agents and have a diameter of 50–300 nm [33].

These nanoparticles can take advantage of leaky vasculature and accumulate in the tumour due to their small size. This so-called EPR effect (enhanced permeability retention) seems especially effective for a tumour with extensive vasculature [34].

Analysis of zeta potential

The assessment of zeta potential values of the formulated TG-NLC formulation is essential in analysing the system's stability throughout extended storage periods. The electrical potential at the particle shear plane is quantified by the zeta potential value. A higher zeta potential value indicates excellent stability in the colloidal system (fig. 4). This increased stability can be attributed to the stronger repulsion between nearby particles that possess identical charges. Consequently, the repulsion inhibits the aggregation of particles.

Efficiency of drug entrapment and capacity for drug loading

The term "entrapment efficiency" (%EE) refers to the proportion of medicine successfully entrapped within the lipid matrix of nanoparticles by the entrapment process. This percentage is expressed as a percentage of the total amount of drug that is introduced during the formulation process of lipid nanoparticles. The term "loading capacity of drug (%DL)" is the percentage of drug content present within lipid nanoparticles about the overall mass of the lipid matrix. This percentage is called the "loading capacity of the drug" [15].

The encapsulation efficiency (EE) values of TG-NLCs are presented in table 3, all of which exceeded 88%. Based on these findings, it appears that the NLC exhibits a favourable capacity to encapsulate TG, which may be a result of the high lipid solubility of TG. This suggests that the lipid modification does not affect the encapsulation efficiency with a drug loading of TG-NLCs. There was no statistically significant difference found in the drug loading (DL) or encapsulation efficiency (EE) between the TG-NLCs.

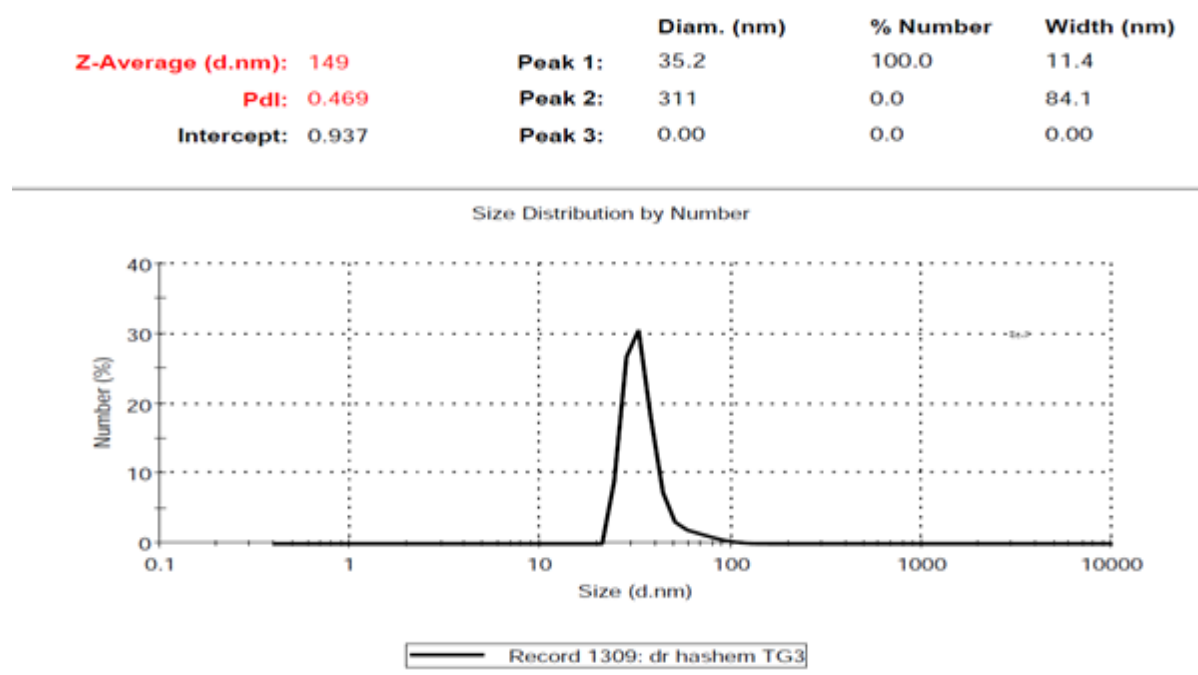


Fig. 3: It shows the DLS-derived size distribution statistics for the chosen formula

Table 2: The values of particle size, PDI, and zeta potential

Code	Particle size	PDI	Zeta (mV)
TG01	510±0.55	0.833±0.002	-24.8±0.42
TG02	379±0.41	0.918±0.003	-24.2±0.23
TG03	149±0.13	0.469±0.002	-13.5±0.27
TG04	192±0.15	0.532±0.003	-11.6±0.15
TG05	201±0.25	0.654±0.004	-10.9±0.29

All data showed mean±SEM (n = 3); n is the number of observations, PDI: Polydispersity Index.

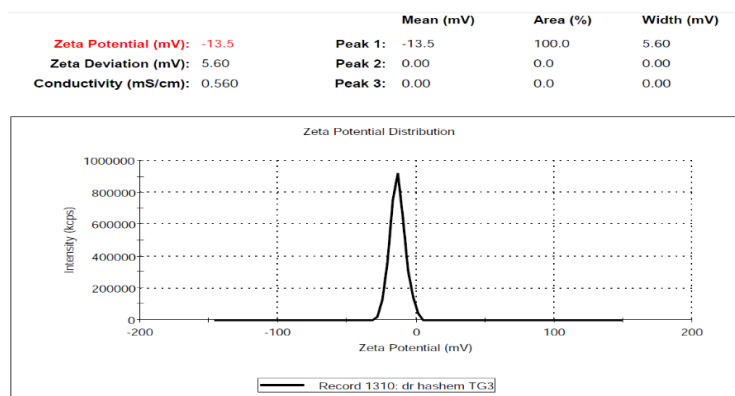


Fig. 4: Illustrates the zeta potential of the chosen formulation, which provides insight into the electric charges exhibited by the produced nanomaterials

Table 3: The drug entrapment efficiency and drug loading capacity percentage

Code	%Entrapment efficiency	%Loading capacity
TG01	94.42±0.35	6.44±0.53
TG02	93.75±0.15	6.53±0.74
TG03	94.87±0.22	6.28±0.37
TG04	88.59±0.51	6.96±0.46
TG05	92.43±0.64	6.35±0.32

All data showed mean±SEM (n = 3), n is the number of observations.

Fourier-transform infrared spectroscopy

The application of FTIR spectral analysis is valuable for assessing the compatibility between drugs and additives and is a crucial aspect in the selection process of excipients. FTIR is employed to investigate potential alterations in the drug molecule throughout the manufacturing process of nanostructured lipid carriers. Fig. 5 (A and B) depict the normal FTIR spectra of thioguanine (TG), as well as the FTIR spectra of pure TG and a physical combination.

As shown in fig. 5B, the absorption bands observed for pure TG exhibited the distinctive characteristics of pure TG. These included peaks at 3285 in addition to 3121 cm^{-1} ; it was by the stretching of the amine group in both asymmetric and symmetric directions. Additionally, absorption bands were observed at 1669 and 1625 cm^{-1} , indicating the presence of C=N and C=C bonds, respectively. Furthermore, a peak at about 1541 cm^{-1} was observed, indicating the presence of C=S stretching groups within the TG range. The bands observed at wavenumbers of around 3284 and 3120 cm^{-1} correspond to the vibrational modes associated with the asymmetrical, symmetrical, and stretching motions of the NH bonds,

respectively. The TG-FTIR spectrum was corroborated by all the other bands.

Fig. 5A demonstrates the FTIR spectra of NLCs. It has been found that there is no perceptible interaction between medicine and the excipients that are being used. The peaks of the drug and the excipient can be distinguished from one another and analysed using the spectrum [35].

Field emission scanning electron microscope

The study involving FESEM was conducted to obtain data regarding the morphology of the TG-NLCs. To mitigate the accumulation of electrostatic charge on the surface, the state of the FESEM must be grounded or conductive.

Fig. 6 of the optimized formula (TG03) exhibits predominantly spherical shapes, with the size of TG-NLCs falling inside the nanoscale scale. Based on the FESEM image analysis of the TG-NLCs, it was observed that the samples exhibited a uniform distribution and spherical morphology, indicating a well-dispersed nature of NLCs.

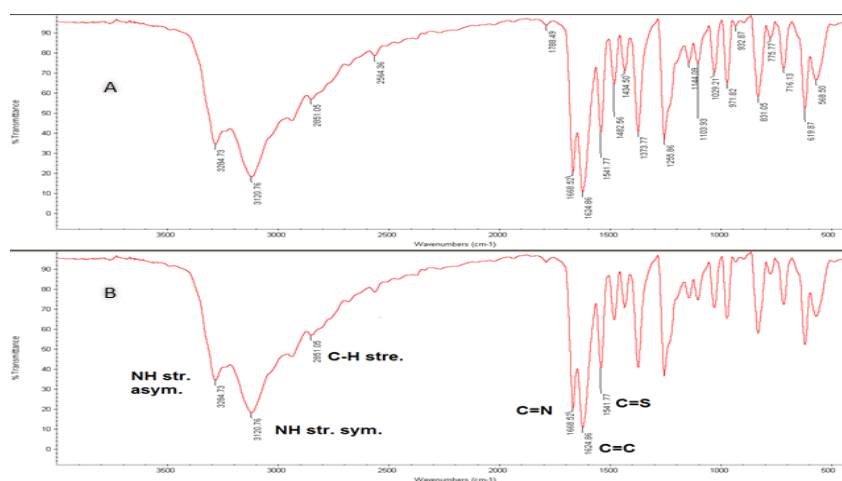


Fig. 5: Displays the fourier-transform infrared spectra of (A) a physical mixture of TG-NLCs and (B) pure thioguanine

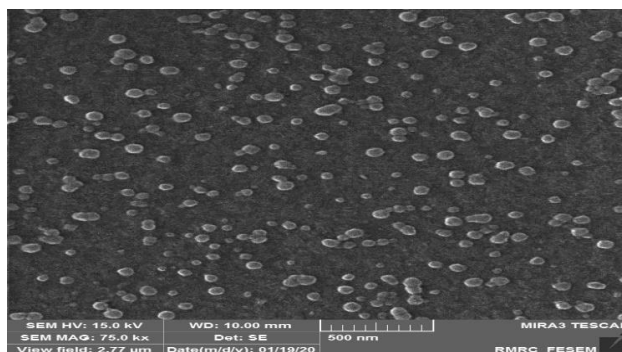


Fig. 6: Displays the field emission scanning electron microscopy images of the thioguanine analysis of the selected formula of nanostructured lipid carriers

***In vitro* release of thioguanine-loaded nanostructured lipid carriers**

In this study, we examined the impact of NLCs on the liberation of thioguanine by an *in vitro* approach, utilising a dialysis bag to measure drug release. The release of TG from the NLC system, as seen *in vitro*, ranged from around 45.72% to 71.92% after 48 h, as shown in table 4 and fig. 7. The release rate of TG from all NLCs varied significantly depending on the mix of oil and lipid phases.

In a prior study, it was reported that the release of TG from TG01 was lower compared to that from a lipid emulsion, with levels ranging from around 1.60% to 11.38% at 48 h [36].

The typical release profile exhibits two distinct phases, namely an initial burst release (seen in TG01 and TG05) attributed to the drug residing on the surface of the nanoparticles, after which there is a continuous release of the medication from the core component [37].

The utilisation of lecithin has been found to promote attachment, leading to more rapid degradation compared to steric stabilisers like poloxamers. This is due to the steric hindrance caused by

poloxamers, which impedes the attachment process and hence slows down the degradation, as documented in previous studies.

Furthermore, it was discovered that the rate of TG release was significantly influenced by the specific oil phase employed. The observed phenomenon may be attributed to the inclusion of solid lipids, specifically Compritol® and CP. The combination of melted solid lipids and liquid lipids resulted in an elevated viscosity of the particles, thereby causing a decelerated release rate [38]. The findings of this study provide evidence that the integration of TG into NLCs is more advantageous compared to the utilisation of lipid nanoparticle delivery systems. Furthermore, the absence of any abrupt release of drugs in TG03 suggests the potential for sustained release of TG from lipid nanoparticle delivery systems.

Cytotoxicity assessment

In this study, the efficiency of TG-NLCs in MCF-7 breast cancer cells was studied *in vitro* by MTT assay. Firstly, the IC_{50} was 1.75 µg/ml, and the range of free TG was between 1 and 5 µg/ml, with a cell viability mean of 53% and 40%, respectively, as shown in table 5 and fig. 8.

Table 4: The cumulative amount of TG (TG01-TG05) in phosphate buffer with a pH of 7.4, at a temperature of 37 ± 0.5 °C

	TG01	TG02	TG03	TG04	TG05
Time (h)	Concentration (µg/ml)				
2	9.47±0.07	8.35±0.10	5.76±0.05	4.71±0.10	8.95±0.03
4	12.83±0.11	11.23±0.16	10.06±0.19	8.92±0.12	11.45±0.08
8	18.34±0.13	16.81±0.12	16.08±0.13	19.73±0.16	20.22±0.11
12	21.69±0.24	22.74±0.11	22.32±0.20	26.22±0.14	24.81±0.28
18	25.46±0.09	27.66±0.08	33.62±0.11	33.49±0.19	22.98±0.13
24	27.51±0.21	32.92±0.22	37.87±0.16	35.78±0.22	25.46±0.24
36	32.55±0.18	44.52±0.14	51.32±0.09	52.59±0.20	39.52±0.18
48	45.72±0.27	54.12±0.17	71.92±0.21	67.27±0.25	57.13±0.23

All data showed mean±SEM (n = 3); n is the number of observations.

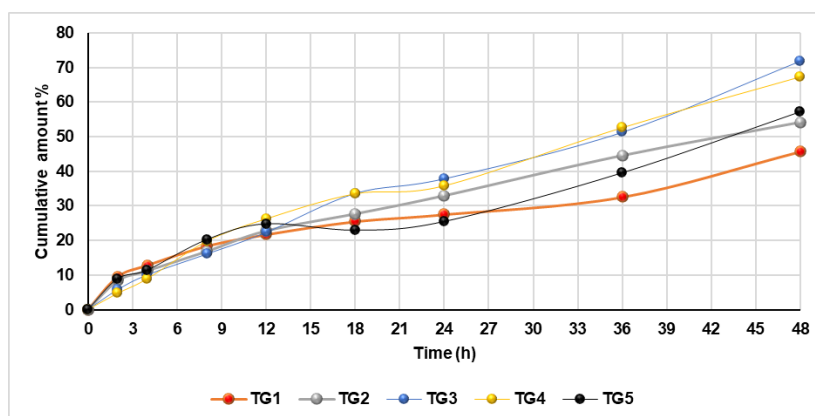


Fig. 7: The cumulative amount percent of TG (TG01-TG05) in phosphate buffer with a pH of 7.4, maintained at a temperature of 37 ± 0.5 °C. Error bars are omitted

Table 5: The cell viability percentages of concentrations of free TG

Concentration ($\mu\text{g/ml}$)	0	0.1	0.5	1	5	10	50	100
	103.69	85.97	60.38	51.84	37.75	36.43	22.33	19.37
	98.39	83.89	58.93	53.49	39.69	36.36	21.87	18.77
	97.93	84.98	59.91	53.49	41.77	32.91	19.76	18.58
Mean	100	85	60	53	40	35	21	19
SEM	1.85	0.60	0.43	0.55	1.16	1.16	0.79	0.24

$n = 3$, n is the number of observations.

The MTT assay has evaluated TG cytotoxicity in the MCF-7 cell line. The cellular toxicities of free TG, blank NLCs, and TG-NLCs were

investigated on the MCF-7 cell line at TG of 1, 2, and 5 $\mu\text{g/ml}$ and were incubated for 72 h (fig. 9).

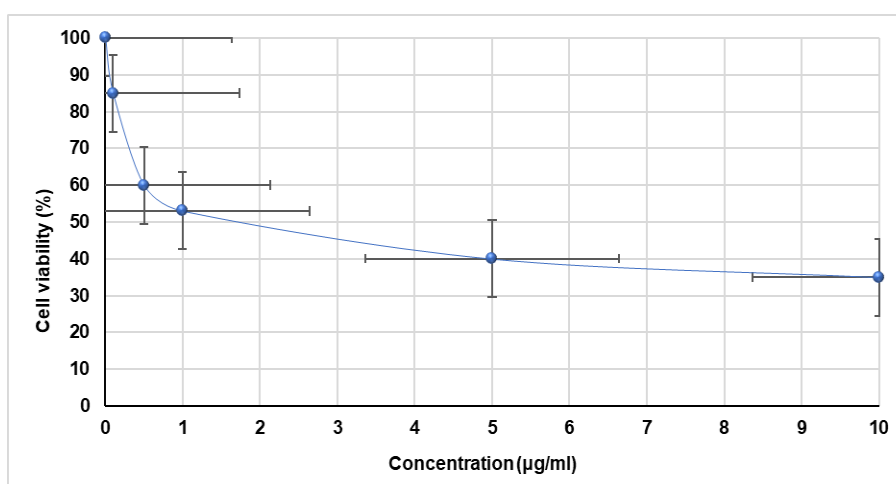


Fig. 8: Illustrates the impact of varying concentrations of unbound medication on the survival rate of the MCF-7 cell line over 72 h of exposure. The data are presented as the mean \pm SEM ($n = 3$)

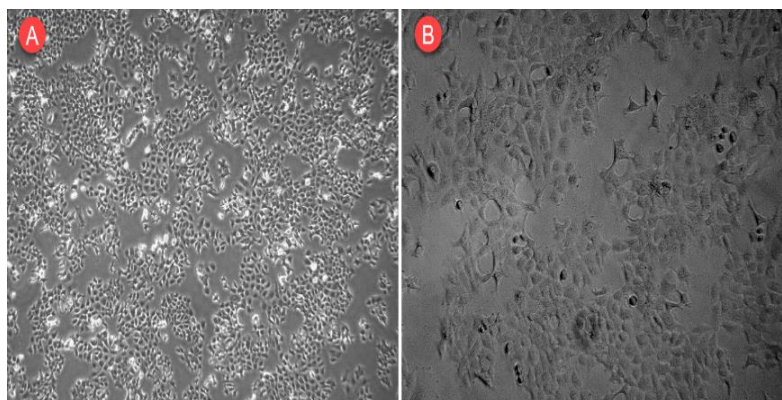


Fig. 9: Exhibits the morphological properties of MCF-7 cells, with the magnification of the A and B images being $\times 4$ and $\times 10$, respectively

The cytotoxicity of TG-NLCs and blank NLCs in comparison to free TG at equivalent concentrations (fig. 10). The anti-proliferation properties of both free TG and TG-NLCs were evaluated in cell culture research using MCF-7 cells. A notable decrease in cell proliferation was seen when the MCF-7 cell line was treated with TG-NLCs, as compared to the control experiment. Nevertheless, the findings indicated a significant decrease in the proliferation of MCF-7 cancer cells when exposed to concentrations of 1, 2, and 5 $\mu\text{g/ml}$ of TG-NLCs.

In the present investigation, as indicated in table 6, a statistically significant difference was observed in the concentration of free TG and TG-NLCs in each concentration. The results demonstrate that both free TG and TG-NP exhibit dose- and time-dependent anti-proliferation effects on this particular cancer cell line. Furthermore,

TG-NLCs exhibit a much higher level of anti-proliferation action compared to free TG across all incubation doses. In general, this work confirms that the use of TG-NLCs considerably enhances anti-proliferation activity.

The absorption of TG-NLCs by MCF-7 cancer cells could be enhanced by electrostatic contact [31]. As previously documented [24], nanoparticles possess an inherent resemblance to several biological entities at the nanoscale, including proteins, viruses, and cellular components.

This similarity enables their internalisation and subsequent transportation to the lysosomes, where they undergo digestion [39]. Similarly, the MCF-7 cell line can internalise TG-NLCs by engulfment and subsequent transport to the lysosome. Within the lysosome's

low pH environment, the thiol group of TG becomes protonated, resulting in the distribution of complementary medication. The

unbound medication subsequently permeates the cell in a manner that is comparable to the diffusion of unbound TG [40].

Table 6: Cytotoxicity of both free drug and TG-NLCs on the MCF-7 cell line following a 72-hour exposure period

Formula	Blank				Free drug			TG-NLCs		
	Control	P1	P2	P5	D1	D2	D5	TG1	TG2	TG5
	100.52	73.72	69.16	68.8191	52.73	51.33	42.13	36.11	29.36	25.90
	101.16	74.70	69.16	66.07	56.39	50.92	44.40	36.90	29.51	25.67
	98.33	74.78	73.76	72.63	50.70	47.98	39.87	35.31	29.06	26.23
Mean	100	74	71	69	53	50	42	36	29	26
SEM	0.86	0.34	1.53	1.9	1.67	1.06	1.31	0.46	0.13	0.16

n = 3; n is the number of observations.

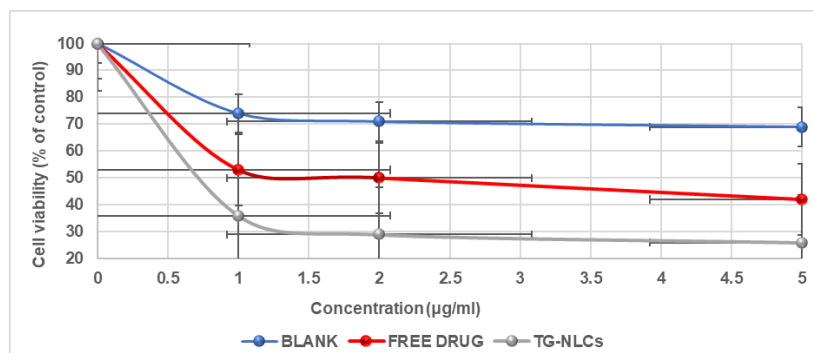


Fig. 10: The cytotoxicity of both the free drug and TG-NLCs on the MCF-7 cell line over a 72-hour exposure period. The data are presented in the form of a mean±SEM with a sample size of n = 3

CONCLUSION

In this study, the anti-proliferation properties of free TG and TG-NLCs against the MCF-7 breast cancer cell line were investigated and compared. The results demonstrated that NLCs considerably improve TG's anti-proliferation activity, which could be due to increased intracellular uptake of this drug via the endocytosis mechanism. As a result, the increased anti-proliferation efficacy of TG via NLC carriers may allow for a reduction in overall drug concentration, renal clearance, and side effects during cancer treatment.

ACKNOWLEDGMENT

The authors express their deep appreciation to the Nanotechnology Research Centre (NRC) of Tehran University of Medical Sciences (TUMS) for providing the laboratories and equipment needed to complete this study.

FUNDING

Nil

AUTHORS CONTRIBUTIONS

All authors, Alaa A. Hashim, Dhiya Altememy, Hussein A. Mohammad, Hasanain S. Mahmood, Radhwan M. Hussein, Mahsa Rezaei, and Pegah Khosravian, have contributed equally to the development and execution of this work. Each author actively participated in the conceptualization, data collection, analysis, and manuscript preparation. All authors have reviewed and approved the final version of the manuscript for publication.

CONFLICTS OF INTERESTS

Declared none

REFERENCES

- Mosleh Shirazi S, Abbasi M, Moaddeli MR, Vaez A, Shafiee M, Kasraee SR. Nanotechnology advances in the detection and treatment of cancer: an overview. *Nanotheranostics*. 2022;6(4):400-23. doi: 10.7150/ntno.74613, PMID 36051855.
- Karimi Maleh H, Fallah Shojaei A, Karimi F, Tabatabaieian K, Shakeri S. Au nanoparticle loaded with 6-thioguanine anticancer drug as a new strategy for drug delivery. *J Nanostruct*. 2018;8(4):217-424.
- Martindale BA. The complete drug reference. 39th ed. UK: Pharmaceutical Press; 2017. p. 871.
- Luengo A, Gui DY, Vander Heiden MG. Targeting metabolism for cancer therapy. *Cell Chem Biol*. 2017;24(9):1161-80. doi: 10.1016/j.chembiol.2017.08.028, PMID 28938091.
- Ford LT, Berg JD. Thiopurine S-methyltransferase (TPMT) assessment prior to starting thiopurine drug treatment; a pharmacogenomic test whose time has come. *J Clin Pathol*. 2010;63(4):288-95. doi: 10.1136/jcp.2009.069252, PMID 20354201.
- Selvamuthukumar S, Velmurugan R. Nanostructured lipid carriers: a potential drug carrier for cancer chemotherapy. *Lipids Health Dis*. 2012;11(1):159. doi: 10.1186/1476-511X-11-159, PMID 23167765.
- Elmowafy M, Al-Sanea MM. Nanostructured lipid carriers (NLCs) as drug delivery platform: advances in formulation and delivery strategies. *Saudi Pharm J*. 2021;29(9):999-1012. doi: 10.1016/j.jsps.2021.07.015, PMID 34588846.
- Beale JM, Block JH. Organic medicinal and pharmaceutical chemistry. 12th ed. Wolters Kluwer Health; 2011. p. 378.
- Convention USP U. S. Pharmacopoeia 2020. USP. NF 38 Convention. Vol. 43. United States Pharmacopoeial; 2020. p. 6497.
- Grabowska Jadach I, Drozd M, Kulpińska D, Komendacka K, Pietrzak M. Modification of fluorescent nanocrystals with 6-thioguanine: monitoring of drug delivery. *Appl Nanosci*. 2020;10(1):83-93. doi: 10.1007/s13204-019-01101-6.
- Gilda SS, Kolling WM, Nieto M, McPherson T. Stability and beyond-use date of a compounded thioguanine suspension. *J Pharm Technol*. 2021;37(1):23-9. doi: 10.1177/8755122520952436, PMID 34752544.
- Huang R, Li J, Kebebe D, Wu Y, Zhang B, Liu Z. Cell penetrating peptides functionalized gambogic acid-nanostructured lipid carrier for cancer treatment. *Drug Deliv*. 2018;25(1):757-65. doi: 10.1080/10717544.2018.1446474, PMID 29528244.
- Gao W, Meng T, Shi N, Zhuang H, Yang Z, Qi X. Targeting and microenvironment-responsive lipid nanocarrier for the

- enhancement of tumor cell recognition and therapeutic efficiency. *Adv Healthc Mater.* 2015;4(5):748-59. doi: 10.1002/adhm.201400675, PMID 25522298.
14. Ma Z, Li N, Zhang B, Hui Y, Zhang Y, Lu P. Dual drug-loaded nano-platform for targeted cancer therapy: toward clinical therapeutic efficacy of multifunctionality. *J Nanobiotechnology.* 2020;18(1):123. doi: 10.1186/s12951-020-00681-8, PMID 32887626.
 15. Shinde AJ, Tarlekar SD, Jarag RJ, Tamboli FA. Antipsoriatic activity of hydrogel containing nanostructured lipid carrier (Nlc) entrapped with triamcinolone acetonide. *Int J App Pharm.* 2023;15(1):308-17. doi: 10.22159/ijap.2023v15i1.46198.
 16. Kesharwani R, Patel DK, Yadav PK. Bioavailability enhancement of repaglinide using nano lipid carrier: preparation characterization and *in vivo* evaluation. *Int J App Pharm.* 2022;14(5):181-9. doi: 10.22159/ijap.2022v14i5.45032.
 17. Dong Z, Iqbal S, Zhao Z. Preparation of ergosterol-loaded nanostructured lipid carriers for enhancing oral bioavailability and antidiabetic nephropathy effects. *AAPS PharmSciTech.* 2020;21(2):64. doi: 10.1208/s12249-019-1597-3, PMID 31932990.
 18. Alhamdany AT, Abbas AK. Formulation and *in vitro* evaluation of amlodipine gastroretentive floating tablets using a combination of hydrophilic and hydrophobic polymers. *Int J App Pharm.* 2018;10(6):126-34. doi: 10.22159/ijap.2018v10i6.28687.
 19. Tekade RK. Basic fundamentals of drug delivery. Academic Press; 2018. p. 369-400.
 20. Aghevlian S, Yousefi R, Faghihi R, Abbaspour A, Niazi A, Jaberipour M. The improvement of anti-proliferation activity against breast cancer cell line of thioguanine by gold nanoparticles. *Med Chem Res.* 2013;22(1):303-11. doi: 10.1007/s00044-012-0030-1.
 21. Hasanzadeh D, Mahdavi M, Dehghan G, Charoudeh HN. Farnesiferol C induces cell cycle arrest and apoptosis mediated by oxidative stress in MCF-7 cell line. *Toxicol Rep.* 2017;4:420-6. doi: 10.1016/j.toxrep.2017.07.010, PMID 28959668.
 22. Rahman HS, Rasedee A, How CW, Abdul AB, Zeenathul NA, Othman HH. Zerumbone-loaded nanostructured lipid carriers: preparation, characterization, and antileukemic effect. *Int J Nanomedicine.* 2013;8:2769-81. doi: 10.2147/IJN.S45313, PMID 23946649.
 23. Aykul S, Martinez Hackert E. Determination of half-maximal inhibitory concentration using biosensor-based protein interaction analysis. *Anal Biochem.* 2016;508:97-103. doi: 10.1016/j.ab.2016.06.025, PMID 27365221.
 24. Chatterjee M, Jaiswal N, Hens A, Mahata N, Chanda N. Development of 6-thioguanine conjugated PLGA nanoparticles through thioester bond formation: benefits of electrospray mediated drug encapsulation and sustained release in cancer therapeutic applications. *Mater Sci Eng C Mater Biol Appl.* 2020;114:111029. doi: 10.1016/j.msec.2020.111029, PMID 32994006.
 25. McHugh ML. Multiple comparison analysis testing in ANOVA. *Biochem Med (Zagreb).* 2011;21(3):203-9. doi: 10.11613/bm.2011.029, PMID 22420233.
 26. Budavari S. The merck index: an encyclopedia of chemicals, drugs, and BioLogicals. 11th ed. Merck; 1989. p. 1470.
 27. Castegnaro M, Berek J, Dennis J, Ellen G, Klibanov M, Lafontaine M. Laboratory decontamination and destruction of carcinogens in laboratory wastes: some aromatic amines and 4-nitrobiphenyl. *IARC Sci Publ.* 1985;64:1-85. PMID 4065953.
 28. Li Q, Cai T, Huang Y, Xia X, Cole SPC, Cai Y. A review of the structure, preparation, and application of NLCs, PNPs, and PLNs. *Nanomaterials (Basel).* 2017;7(6):122. doi: 10.3390/nano7060122, PMID 28554993.
 29. Kuo CH, Chiang TF, Chen LJ, Huang MH. Synthesis of highly faceted pentagonal- and hexagonal-shaped gold nanoparticles with controlled sizes by sodium dodecyl sulfate. *Langmuir.* 2004;20(18):7820-4. doi: 10.1021/la049172q, PMID 15323536.
 30. Cho EC, Zhang Q, Xia Y. The effect of sedimentation and diffusion on cellular uptake of gold nanoparticles. *Nat Nanotechnol.* 2011;6(6):385-91. doi: 10.1038/nnano.2011.58, PMID 21516092.
 31. Pan Y, Neuss S, Leifert A, Fischler M, Wen F, Simon U. Size-dependent cytotoxicity of gold nanoparticles. *Small.* 2007;3(11):1941-9. doi: 10.1002/sml.200700378, PMID 17963284.
 32. Gupta S, Kesarla R, Chotai N, Misra A, Omri A. Systematic approach for the formulation and optimization of solid lipid nanoparticles of efavirenz by high pressure homogenization using design of experiments for brain targeting and enhanced bioavailability. *BioMed Res Int.* 2017;2017:5984014. doi: 10.1155/2017/5984014, PMID 28243600.
 33. Haider M, Abdin SM, Kamal L, Orive G. Nanostructured lipid carriers for delivery of chemotherapeutics: a review. *Pharmaceutics.* 2020;12(3):288. doi: 10.3390/pharmaceutics12030288, PMID 32210127.
 34. Nakamura Y, Mochida A, Choyke PL, Kobayashi H. Nanodrug delivery: is the enhanced permeability and retention effect sufficient for curing cancer? *Bioconjug Chem.* 2016;27(10):2225-38. doi: 10.1021/acs.bioconjchem.6b00437, PMID 27547843.
 35. Gunasekaran S, Kumaresan S, Arunbalaji R, Anand G, Seshadri S, Muthu S. Vibrational assignments and electronic structure calculations for 6-thioguanine. *J Raman Spectroscopy.* 2009;40(11):1675-81. doi: 10.1002/jrs.2318.
 36. Ji P, Yu T, Liu Y, Jiang J, Xu J, Zhao Y. Naringenin-loaded solid lipid nanoparticles: preparation, controlled delivery, cellular uptake, and pulmonary pharmacokinetics. *Drug Des Devel Ther.* 2016;10:911-25. doi: 10.2147/DDDT.S97738, PMID 27041995.
 37. Fang CL, Al-Suwayeh SA, Fang JY. Nanostructured lipid carriers (NLCs) for drug delivery and targeting. *Recent Pat Nanotechnol.* 2013;7(1):41-55. doi: 10.2174/187221013804484827, PMID 22946628.
 38. Chinsriwongkul A, Chareanputtakhun P, Ngawhirunpat T, Rojanarata T, Sila-on W, Ruktanonchai U. Nanostructured lipid carriers (NLC) for parenteral delivery of an anticancer drug. *AAPS PharmSciTech.* 2012;13(1):150-8. doi: 10.1208/s12249-011-9733-8, PMID 22167418.
 39. Alkilany AM, Thompson LB, Boulos SP, Sisco PN, Murphy CJ. Gold nanorods: their potential for photothermal therapeutics and drug delivery, tempered by the complexity of their biological interactions. *Adv Drug Deliv Rev.* 2012;64(2):190-9. doi: 10.1016/j.addr.2011.03.005, PMID 21397647.
 40. Podsiadlo P, Sinani VA, Bahng JH, Kam NW, Lee J, Kotov NA. Gold nanoparticles enhance the anti-leukemia action of a 6-mercaptopurine chemotherapeutic agent. *Langmuir.* 2008;24(2):568-74. doi: 10.1021/la702782k, PMID 18052300.